Extensive aging analysis of high-power lithium titanate oxide batteries: Impact of the passive electrode effect

Thomas Bank^{a,b}, Jan Feldmann^{a,b}, Sebastian Klamor^a, Stephan Bihn^{b,c}, Dirk Uwe Sauer^{b,c,d,e}

^aBMW AG, Petuelring 130, 80788 Muenchen, Germany ^bChair for Electrochemical Energy Conversation and Storage Systems, Institute for Power Electronics and Electrical Drives (ISEA), RWTH Aachen University, Jaegerstrasse 17-19, 52066 Aachen, Germany

^cHelmholtz Institute Muenster (HI MS), IEK 12, Forschungszentrum Juelich, 52425 Juelich, Germany

^dInstitute for Power Generation and Storage Systems (PGS), E.ON ERC, RWTH Aachen University, Mathieustrasse 10, 52074 Aachen, Germany

^eJuelich Aachen Research Alliance, JARA-Energy, Templergraben 55, 52056 Aachen, Germany

Abstract

Partial electrification of vehicle drive trains, for example by the usage of 48 V systems, require high-power batteries with extreme robustness to temperatures, current rates and energy throughputs. In this study, the application-relevant lifetime performance of 33 state-of-the-art high-power lithium titanate oxide nickel manganese cobalt oxide (LTO/NMC) cells is measured under cyclic, calendar, and drive cyclic aging regimes. Regular extended check-ups reveal the cell performance in terms of capacity loss and internal resistance increase, which allows for the identification of critical operating conditions. For the first time a passive electrode effect is identified in calendar aging tests of LTO cells in which the cathode is geometrically and capacitively oversized. Passive electrode areas lead to a change in cell balancing, which can be illustrated by the shift of the half-cell voltage curves. Generally, the investigated cells show an excellent cycle stability for shallow cycles, even at high ambient temperatures and high current rates. Only large cycle depths greater than 70% at elevated temperatures reduce the battery life significantly. Furthermore, the results show that cells cycled in areas of low state of charge age faster than in areas of high state of charge. The rise in internal resistance under calendar aging has the most detrimental influence on lifetime in a 48 V battery.

Keywords: Lithium titanate oxide, Aging analysis, Passive electrode effect, 48 V system, High-power

1. Introduction

In order to comply with the recent regulations about exhaust gas and particularly CO₂ emissions car manufacturers are forced to develop new concepts for the electrification of the powertrain. In addition to purely electric vehicles, partially electrified models in the form of plug-in, full hybrid and mild hybrid systems are increasingly en-

Email addresses: thomas.bank@bmw.de (Thomas Bank),

vehicles (MHEV) equipped with a 48 V electrical system are promising for car manufacturers due to their low component costs, good integrability and high effort-to-benefit ratio with regard to CO₂ savings potential [1, 2]. Lithiumion batteries used within a 48 V application are exposed to severe operating conditions, which have been investigated in a previous publication [3]. In addition to high temperatures due to the limited installation space, high current rates of up to 26 C and high energy throughputs over the vehicle lifetime occur. Batteries designed for high power

applications are necessary to meet these requirements. In

tering the vehicle market. Especially mild hybrid electric

jan.feldmann1@rwth-aachen.de (Jan Feldmann), sebastian.klamor@bmw.de (Sebastian Klamor),

stephan.bihn@isea.rwth-aachen.de (Stephan Bihn),

dirkuwe.sauer@isea.rwth-aachen.de (Dirk Uwe Sauer)

particular, the use of LTO as anode material offers advantages. This material, known for its "zero-strain" characteristic, provides extremely high power densities due to its spinel structure and submicrometer particle size [4, 5]. In addition, the high voltage plateau ($\approx 1.55 \,\mathrm{V}$ to Li/Li⁺) significantly reduces the risk of lithium plating. Due to the high potential, almost no solid electrolyte interface (SEI) is formed on the surface of the LTO. For this reason, firstly, no additives are needed to support SEI formation and secondly, it cannot decompose at elevated temperatures [6, 7]. Both these factors lead to a considerably increased temperature stability of LTO, which results in a high level of safety [4, 8, 9]. The low energy density is only of minor importance in high power applications. In general, LTO offers a high cycle stability, although the gassing behaviour at high temperatures can be limiting [10, 11].

In principle, few comprehensive aging studies on LTO cells exist in the literature. Reasons for this are, among others, the low spread of LTO cells in commercial applications and the high price of the material [12]. In addition, aging studies of LTO cells are very time and cost intensive due to high cycle and calendar lifetimes. For this reason, cyclic aging has been accelerated using higher C-rates (2 to 10 C) and temperatures (20 to 55 °C) [10, 13, 14, 15, 16]. All investigations showed a high cycle stability, even at elevated temperatures. Hall et al. [13] and Svens et al. [16] were able to prove that the cathode is the more lifetimecritical material in the examined cells. Calendar aging tests also showed an outstanding lifetime of LTO based cells [16, 17]. Only high temperatures in combination with high states of charge have been found to shorten the battery lifetime due to strong gassing behaviour [18]. On the one hand, this tendency towards gassing is due to parasitic reactions of the LTO with the electrolyte. On the other hand, residual moisture within the electrodes and the electrolyte, which, for example, originates from the process of the cell production, leads to increased gassing. Thus, Fell et al. [18] could prove a correlation between the

residual moisture content and the amount of gas produced within the cell. All investigations existing in the literature consider only single, partly arbitrarily chosen operating parameters for the aging analysis. There is a lack of holistic, multi-dimensional aging measurements that attempts to cover all essential dependencies of the calendar and cyclic aging behaviour of LTO-based cells. In addition, a clear focus on an application-oriented approach with concrete reference to a high-performance application, such as a mild-hybrid system, is needed and necessary.

For this reason, state-of-the-art high power cells are subjected to various aging tests in an application-oriented 48 V context in this work. In particular, the influence of temperature, current rate, state of charge, cycle depth and energy throughput are investigated. The cells show outstanding lifetime performance under synthetic cyclic, calendar and realistic drive cycle conditions. With regard to cyclic load, high cycle depths and the accompanying low and high states of charge lead to most rapid aging. Drive cyclic aging results indicate that the life time requirement of 200.000 km can be met even under high temperature loads. For calendar aging at high temperatures (80 °C) a strong gassing behaviour is observed. Interestingly, in addition to the critical high states of charge frequently reported in the literature, low states of charge also enhance the gas formation in the investigated cells. To our knowledge, this study is the first to report and explain the passive electrode effect (PEE) in cells with a geometrically oversized cathode. The PEE affects the availability of lithium-ions within the active area and thus influences the balancing of anode and cathode. An explanatory model is developed that allows for a differentiation of the consequences of floating and non-floating test conditions. Considering the PEE is particularly important for the study of stable LTO-based cells, in which under normal operating conditions of up to 60 °C hardly any loss of capacity as a result of calendar aging can be observed. Here, neglecting the PEE can lead to significant misinterpretations and

incorrect state-of-health predictions.

The following parts of this paper are organized as follows: Section 2 describes the scope and implementation of the aging tests including the regular check-up. Furthermore, the theory behind the PEE is explained. Based on the extensive aging tests, Section 3 analyses the operating parameters with regard to their impact on the calendar and cyclic cell life. A discussion of the findings and an evaluation of the criticality with respect to a 48 V application conclude this section. Finally, a summary is presented in Section 4 and further research questions are raised.

2. Experimental

In this work the aging behavior of 33 pouch cells was examined. The active material of the investigated 10.6 Ah cells is LTO on anode side and NMC on cathode side. The characteristic open circuit voltage (OCV) curve, measured at 25 °C, is shown in Figure 1a. Compared to cells with graphite anodes, no noticeable plateaus are visible [19]. In terms of active material and electrolyte composition, the cell is designed for extremely high currents and a wide temperature window. The high available pulse currents of more than 50 C in charge and discharge direction are ideal for high power applications, such as a 48 V application in a MHEV. An overview of the data sheet of the cell is given in Table 1.

Table 1: Cell specifications according to the manufacturer's data sheet.

Nominal Capacity [Ah]	10.6
Cell Format	Pouch
Cathode Active Material	NMC
Anode Active Material	LTO
Nominal Voltage [V]	2.2
Upper Voltage Limit [V]	2.65
Lower Voltage Limit [V]	1.9
Max. Pulse Discharge Current ([A], 1s)	760
Max. Pulse Charge Current ([A], 1s)	520
Operating Temperature [°C]	-30 - +70

All cells were tested in between two aluminum bracing plates under the pressure specified by the manufacturer. To increase the accuracy and taking into account the low internal resistance of the cell, all measurements were carried out using a 4-pole measuring principle. The cell temperature was determined using two type K sensor in the middle of the cell and between the cell tabs. For this purpose, the aluminum bracing plates were provided with small cutouts. These cutouts were leveled out with filler to prevent inhomogenities. An overview of the measuring equipment is provided in Table 2.

Table 2: Technical data of the measuring equipment used for the aging tests.

Test routine	Devices	
Checkups	Digatron MCT 300-06-4(3)ME	
Cyclic aging tests	Neware CT-4008-5V $100A$ -NA	
Calendar aging tests	Rohde & Schwarz HMP4040	
Climate chamber	Binder model MK 240	

The calendar, cyclic and drive cyclic aging matrices on which this analysis is based were defined in the work of Bank et al. [3]. For the definition, real-world 48 V battery data were examined and application-specific operating points identified. The aging matrices published by Schmalstieg et al. [20] served as a basis. In addition to the tests defined in [3], further measurements aim to quantify the voltage dependency of the cyclic aging behavior with different cycle depths and average states of charge. These complementary tests were performed with six cells, two per operating condition. In all other tests, one cell is tested due to the availability of test benches and cells. However, high quality and uniformity can be assumed due to the commercial availability of the cell. Therefore, the begin-of-life condition in terms of capacity and resistance of all investigated cells is shown in Figure 1b. Based on the initial capacity, the cells vary by 2.3%. The variation in internal resistance is significantly higher at 17.7%, but within the range specified by the cell manufacturer. No noticeable influence with regard to the following aging

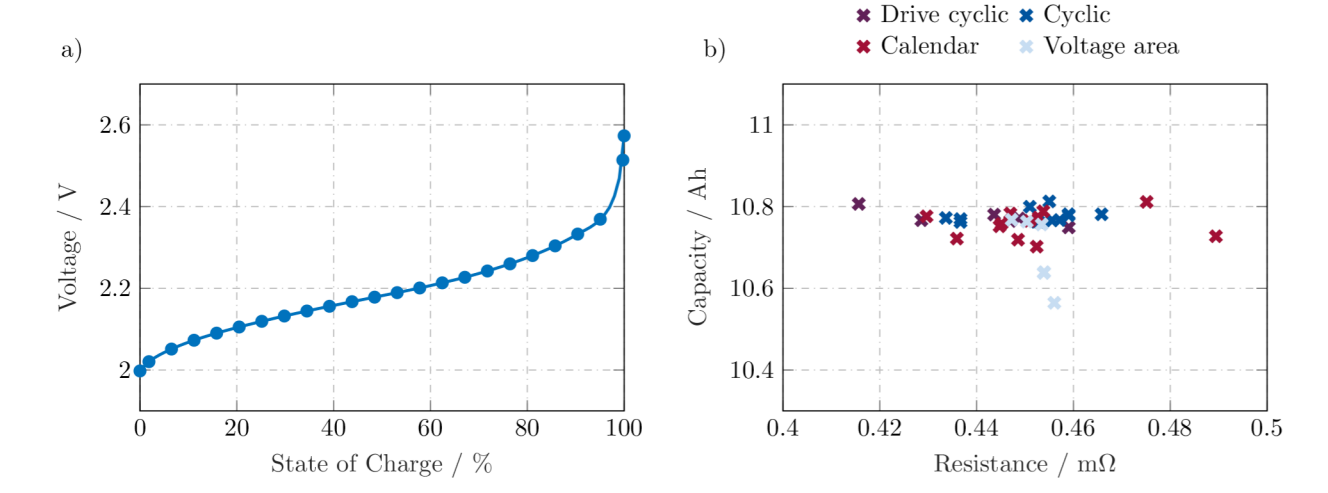


Figure 1: a) OCV curve for a new cell at 25 °C. b) Overview of the performance of all tested cells in terms of discharge capacity (1 C, constant current) and resistance (5 C, 1 s, 50 % SOC) prior to test start. The variation in capacity is much larger than the variation in resistance.

tests could be found. All aging tests were carried out in accordance with the conditions of use specified by the cell manufacturer.

2.1. Calendar aging

The calendar aging tests focus on the investigation of dependencies regarding temperature and state of charge. Both are of particular importance in terms of the underlying 48 V application. In Table 3 the calendar aging matrix is shown. The exclusive consideration of temperatures greater than or equal to 40 °C is due to the conditions within the 48 V application and the limited test time in combination with the excellent life times of LTO cells. A check-up is carried out every 30 days to determine the aging progress. The cell voltage during storage is kept constant. This floating current condition is achieved by a test configuration, which was used similar by Lewerenz et al. [21]. The SOC setting after every check-up is based on the latest measured capacity and is done Ah-based.

2.2. Cyclic and drive cyclic aging

The cyclic aging tests aim to investigate dependencies with respect to cycle depth and current rate. An overview of all test conditions is shown in Table 4. The mean SOC

Table 3: Defined calendar aging matrix based on the investigation of the real-world $48\,\mathrm{V}$ system data.

T/SOC	5%	20%	55%	70%	90 %	95%
40 °C	X		X			X
$60^{\circ}\mathrm{C}$	X	X	X	X	X	X
$80^{\circ}\mathrm{C}$	X		X			X

for all cycle depths smaller than $100\,\%$ is $55\,\%$ and is approached via constant-voltage step. Cyclization around this SOC takes place Ah-based, with a reset of the mean SOC every 20 equivalent full cycles. All cyclization profiles consist exclusively of constant-current charging and discharging processes. The asterisk (*) indicates an operating point at which two cells are tested. One cell is cycled at $5\mathrm{C}/5\mathrm{C}$ and $70\,\%$ cycle depth. The load profile of the other cell is expanded by a sawtooth profile, so that every change of $4\,\%$ state of charge is superimposed by a microcycle of $2\,\%$ in the opposite direction. The aim is to get a better understanding of overlapping aging effects and to generate essential knowledge regarding battery lifetime in dynamic real-world applications. After every 500 equivalent full cycles a check-up is performed.

In addition, as mentioned above, further cyclic aging tests have been defined to investigate the criticality of the

Table 4: Cyclic aging matrix based on the investigation of the real-world $48\,\mathrm{V}$ system data. Cyclization at cycle depths less than $100\,\%$ takes place at an average SOC of $55\,\%$. At (*) an additional cell is loaded with a sawtooth profile, which overlaps a microcycle of $2\,\%$ every $4\,\%$ SOC change.

Current	2C,	/2C	5C,	/5C	10C,	/10C
$\Delta { m DOD/T}$	40 °C	60°C	40 °C	60 °C	40 °C	60 °C
100%			X			
70%	X		X	X^*		
20%			X			
10%			X			
5%	X		X	X		X
2%			\mathbf{X}			

upper and lower voltage ranges. For this purpose, 6 cells, 2 per test condition, were cycled in different voltage windows at 5C/5C and 60 °C. The test conditions can be taken from Table 5. Every 250 cycles the cell performance was checked using a shortened checkup. The general sequence of the checkups and the differences are described in the following section.

Table 5: Additional cyclic aging tests to investigate the aging behavior at low and high states of charge in combination with different cycle depths. The listed charge and discharge voltages define the limits of the constant current step.

U_{lower}/U_{upper}	$2.4\mathrm{V}$	$2.5\mathrm{V}$	$2.65\mathrm{V}$
$2.0\mathrm{V}$	X		
$2.1\mathrm{V}$		X	X

To validate the cyclic and calendar aging tests and for a realistic prognosis regarding the battery lifetime within a 48 V application, 3 cells are loaded with a driving cycle at different temperatures. The cycle includes a combination of real battery loads during city, country and highway driving and has a duration of 16 hours. With the variable temperature profile a temperature level between 20 and 60 °C is set weekly. A total of 10 temperature levels are tested with an average temperature of 37.3 °C. As Ah neutrality cannot be guaranteed due to the cycle itself and measurement inaccuracies, a SOC reset is performed after each drive cycle. A checkup is performed every 32

cycles. The results of the drive cyclic aging can be used in a further step for the verification of an aging model, even though this is not content of this work.

Table 6: The drive cyclic aging profile is based on real-world 48 V battery data. The superimposed variable temperature profile consists of 10 temperature stages between 20 and 60 °C, which are changing weekly.

T 40°C	60 °C	variable
--------	-------	----------

2.3. Check-ups

Check-ups are carried out at defined intervals to monitor the aging behaviour. The entire measurement routine is carried out at 25 °C. An exemplary voltage curve of a check-up is shown in Figure 2. At the beginning of the check-up, the examined cell is charged with a constant current of 1 C to 2.65 V followed by a constant voltage step until the current falls below 1/50 C. Then a capacity test is performed in discharge and charge direction with a constant current of 1 C, concluded with a constant voltage step. A quasi-OCV (qOCV) at 1/8 C is performed for further electrical studies, followed by another capacity test at 1 C [22]. The deviations from the qOCV to a real OCV can be assumed to be very small considering the low current rate in combination with the extremely low internal cell resistance [23].

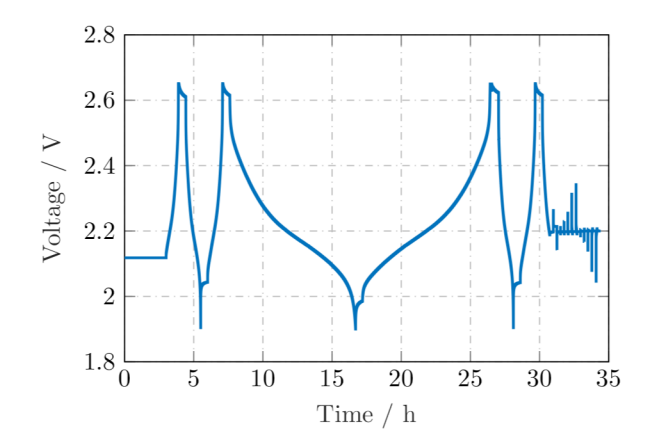


Figure 2: Exemplary voltage profile of a cell during the check-up.

At 50 % SOC a pulse power characterization profile (PPCP) is carried out. First, a charge and a discharge pulse are applied to the cell for 20 seconds with a 15 minute rest in between. After another 15-minute rest period, a sequence of charge and discharge pulses with current rates of 2C, 5C, 10C, 20C and 25C and a pulse duration of 10 seconds is applied with a directly connected equalizing charge of 1 C. The relaxation time between the respective pulses is 15 minutes. In this work the analysis of the internal resistance increase is based on the 5 C pulse behaviour, which is evaluated after 1s pulse duration. To calculate the internal resistance, the difference between the cell voltage before the pulse and 1s after the start of the pulse is divided by the applied current. All data concerning the capacity retention refer to the usable capacity in the first capacity test in discharge direction within the constant current phase.

3. Results and discussion

The following chapter shows the results of a subset of the aging tests described above. Due to the large number of tests and the high cycle and temperature robustness of LTO-based cells, only results important and meaningful for the analysis are shown. Furthermore, the reported findings are primarily empirical, thus concrete correlations between performance data and ageing mechanisms can only be addressed by subsequent, separate investigations. For a general, comprehensive overview of possible aging processes and their effects on cell performance, please refer to the following reviews [24, 25, 26].

3.1. Calendar aging

SOC dependence. With regard to capacity retention over aging, the examined cells exhibit a strong dependence on the storage SOC at which the test was performed. Figure 3a shows the remaining capacity of the cells stored at 60 °C and different SOC. During the first check-up, a delta of 4% between the best (5% SOC) and worst (95% SOC)

performing cell is found with respect to the initial capacity. Up to a test duration of about 100 days this difference increases and reaches a maximum value of over 5%. The difference in capacity is larger than the 2.3% spread of cell capacity at the beginning of the tests. Especially the rise of usable capacity cannot be explained by common aging mechanisms. The sequence of the residual capacity curves corresponds in exact order to the storage SOCs under floating conditions. Over the period under consideration, low SOCs lead to an increase and high SOCs to a decrease in residual capacity. Considering the aging trend over time, the LTO/NMC cells behave very stable despite high temperatures and perform significantly better than other cells reported in the literature [15]. Even after more than 300 days, no degradation behaviour in terms of capacity is recognizable in cells with a SOC smaller than 70%. The results illustrate the challenge of aging tests of LTO-based cells in terms of time requirements and speedup possibilities.

Regarding the internal resistances, as shown in Figure 3b, an increase between 6 to 14.5 % is observed. Here, the internal resistances of the cells with medium SOC have increased the most and those of the cells with low SOC the least. It is difficult to make a general statement regarding this observation, since the deviations between the individual cells with similar SOC are high and measurement inaccuracies due to the very low internal resistances of high-power cells may have a great influence. Nevertheless, the calendar aging tests at 60 °C emphasize that the cells are very well suited for applications where high temperatures over long periods of time occur. Under the assumption of an end of life at 150% relative internal resistance and a linear aging trend, a battery life of 3 years is realistic. A conspicuous gassing behaviour could not be determined, but is difficult to detect optically due to the test setup and is not subject of this work.

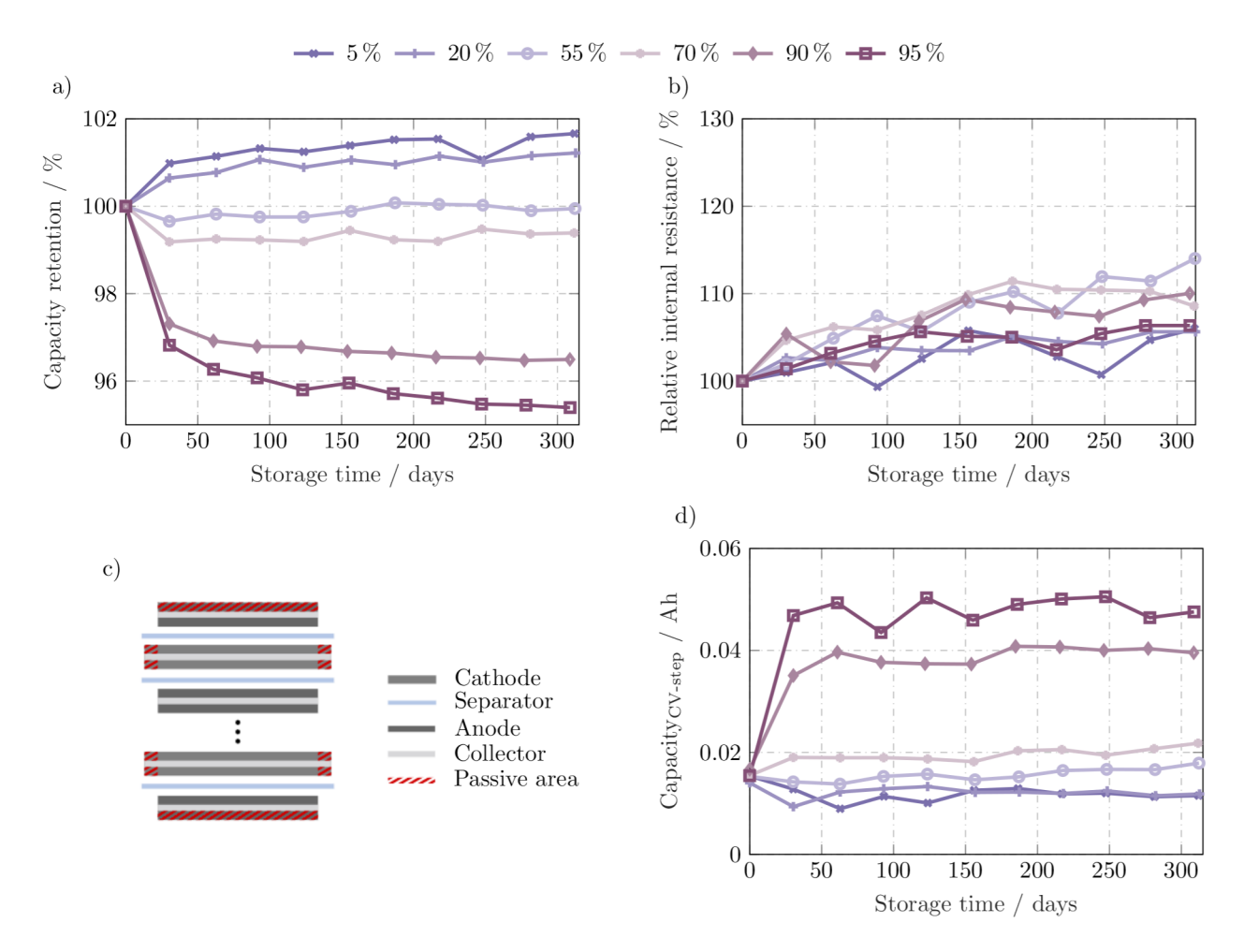


Figure 3: a) Normalized capacity over time and b) normalized resistance over time for calendar aging tests at 60 °C and different SOC. Depending on the storage SOC during the aging tests, the remaining capacity in the first check-up changes significantly. High SOCs lead to a decrease and small SOCs cause an increase of the residual capacity. Only for cells with 90 % and 95 % an approximately linear ageing behaviour is observed after 50 days. The internal resistance of all cells increases, but no distinct SOC-dependent differences can be identified. c) Schematic representation of the geometric arrangement within the cell. The cathode is geometrically oversized on all sides compared to the anode. All sheets are coated on both sides, whereby anode sheets represent the first and last layer of the cell. All areas that are not actively involved in charge and discharge processes are declared as passive areas. d) Capacity added in the CV step of the charging step of the first capacity test. With increasing storage SOC, this capacity rises sharply. Decisive for the magnitude is the homogeneity of the lithiation of the cathode.

3.1.1. Passive electrode effect

Several aging studies in the past showed unexpected capacity rises and drops in the first check-ups, similar to those described above. The large majority of these phenomena can be explained by the anode overhang or, in a broader sense, the PEE, which has already been postulated by various authors [27, 28, 29]. According to these publications, this effect occurs if the graphite anode is ge-

ometrically oversized compared to the opposing cathode. This dimensioning provides a reserve in case of production-related inaccuracies, for example during the stacking process of the electrodes [30]. It ensures that the cathode is always opposite an anode area. Thus, the danger of lithium plating due to excessive accumulation of lithium-ions in the edge areas is reduced [27]. However, the overlapping passive anode material can cause lithium-ion flow from the

active to the passive area and vice versa. The strength and direction of this balancing process depends on the voltage difference between the two areas. Depending on the halfcell potential of the graphite and the location on a plateau or a variable flank, different gradients occur. As a result, the lack or excess of lithium-ions in the active area of the anode lead to a decrease or increase in usable capacity. This effect is completely reversible, since these lithiumions are available for further intercalation processes.

The cell investigated in this work represents a novelty and thus an extension of the prevailing theory in two aspects. In Figure 3c a schematic illustration of the inner cell geometry is shown. A distinction is to be made between two different areas which do not actively participate in charge and discharge processes and thus also in capacity determination. On the one hand there is an edge area of the cathode, which is directly connected to the active area of the cathode and is a few millimeters wide. Since LTObased cells exhibit an extremely low lithium plating risk and LTO material is likely to be more costly than NMC material, the anode is dimensioned smaller. On the other hand, double-sided coated anode sheets are used within the whole cell. Therefore, the anode side facing the pouch foil at the beginning and end of the cell stack is only indirectly involved in the lithiation processes. Based on the geometric conditions within the cell, the anode and cathode overhang result in different diffusion paths for equalization processes. Within the cathode the diffusion path into the passive region is short, whereas large distances of several centimeters must be bridged by solid and electrolyte diffusion in the case of the anode. This leads to the assumption that two individual time constants result for the speed of the compensation processes.

As can be deducted from the data in Figure 3, the impact of the PEE is quite large for the given cell. According to the formula published by Lewerenz et al. [28],

the following value results for the cathode overhang:

Share of
$$PE_{Cathode} = \frac{A_{C_{active passive}}}{A_{C_{active}}} - 1 \approx 5.4\%$$
 (1)

Here A_{Cactive passive} refers to the total area and A_{Cactive} to the active area of a cathode sheet. The anode overhang can be calculated by the ratio of numbers of anode sheets

 $N_{A_{sheets}}$ and cathode sheets $N_{C_{sheets}}$:

Share of
$$PE_{Anode} = \frac{N_{A_{sheets}}}{N_{C_{sheets}}} - 1 \approx 2\%$$
 (2)

How these overhangs affect the capacitive performance of the cells is shown qualitatively in Figure 4 using the halfcell voltage curves. As with the tested cells, a completely relaxed system with approximately 30 % SOC is assumed as initial condition. The adjustment of the storage SOC to 95 % only affects the active areas of cathode and anode at first. The concentration and voltage gradient between the active and passive regions of the cathode results in a balancing ion flow, which increases the charge of the active cathode material. A distinction must be made in this context between calendar aging tests under floating and non-floating condition. Since there is an electrical connection between the anode and cathode in the case of floated cells, an external current flow can occur. As the potential of the active cathode area decreases, the potential and thus the state of charge of the anode must increase to maintain the externally applied full cell voltage. This takes place via a current flow from anode to cathode respectively an ion flow from cathode to anode, which is monitored as floating current. The entire process leads to a change in charge of anode and cathode, which corresponds to a shift of the half-cell voltage curves. This shift, taking into account the upper and lower cell voltage limits, leads to significantly lower extractable capacity in the second check-up. In the case of non-floating test conditions, the equalization process only takes place on the cathode side, thus causing a shift of the half-cell potential. However, this ultimately has similar effects on the available cell capacity.

The overall influence of the passive area of the anode is most likely to be low, not only because of the small propor-

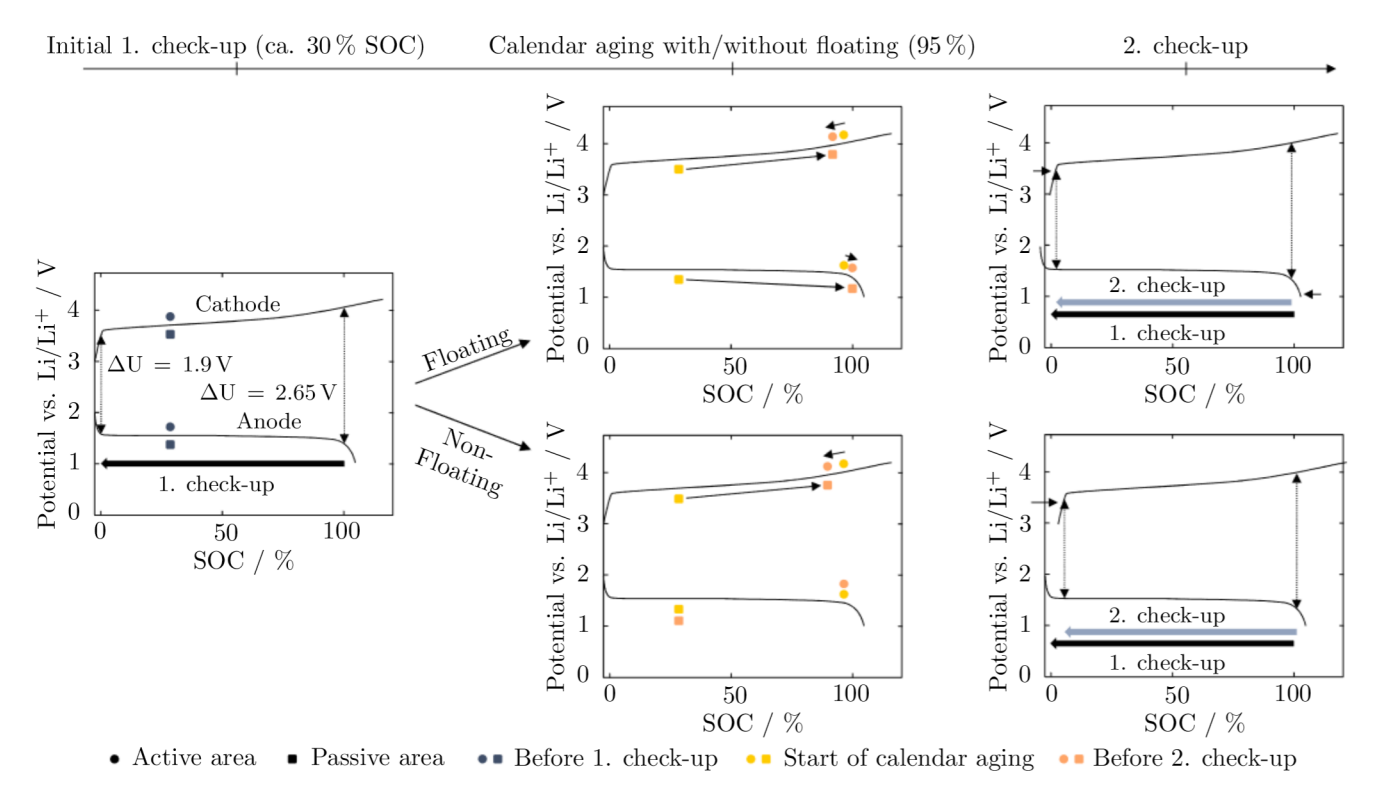


Figure 4: Qualitative explanation for the influence of the passive areas on the resulting discharge capacities in the first and second check-up using anode and cathode potential curves. A fully relaxed system is assumed for the first check-up. At the beginning of calendar aging the examined cells are at approximately 30 % SOC. An increase of the cell SOC leads to a concentration and voltage gradient between the active and passive area and a lithium-ion flow from the passive to the active area. Depending on the test procedure (floating, non-floating), one or both potential curves shift and thus reduce the discharge capacity in the defined operating voltage window.

tion of 2%. On the one hand, the potential of the LTO is nearly constant over the entire operating window, so that balancing processes between the active and passive areas of the anode are small. On the other hand, the aforementioned long diffusion paths have an inhibiting effect.

The half-cell voltage curve of the cathode is decisive for the majority of the equalization processes within the cell. Since NMC vs. Li/Li⁺ has no potential plateaus compared to graphite considered in previous works, the influence increases strictly monotonically with increasing difference between storage SOC before test and during test [28, 29]. This results in a distinct arrangement of the capacity curves for the examined cells according to their storage SOCs during the test. As becomes apparent from the level of the capacity differences and the corresponding SOC level, the intensity increases in the higher SOC

boundary area, where the OCV of the full cell has a steep gradient.

Additionally, the passive area of the cathode has an effect on the homogeneity of the degree of lithiation of the active cathode area. An indicator of this is the capacity that is charged into the cell during a constant voltage phase. In Figure 3d the capacity measured in the constant voltage phase of the charge in the first capacity test of the check-up are illustrated for the calendar aging tests at 60 °C. For all cells nearly identical values can be observed in the first check-up due to the similar SOC start value. From the second check-up onwards, depending on the storage SOC large differences in CV capacities are observed. Particularly noticeable are high storage SOCs, which require the largest CV phase. This can be explained by the degree of lithiation of the passive cathode area. For the

calendar aging test with high SOC, the degree of lithiation of the passive cathode regions is low. During the capacity test the anode is discharged and the active area of the cathode is charged. Due to the high potential difference between lithiated and delithiated cathode material, the passive edge region of the cathode facing the active region is slightly charged. In addition, during the 30-minute break, further ions diffuse into the passive area, further reducing the degree of lithiation in the edge area of the active NMC part and thus increasing the inhomogeneity. During the subsequent charging phase, the anode cannot be lithiated over its entire surface until the cut-off voltage is locally reached, so that a more extensive CV phase is necessary. As Grimsmann et al. [31] theoretically explained for graphite-based cells as well as demonstrated by cell openings, these local inhomogeneities in the active edge areas of the graphite material can lead to lithium plating and thus to significantly shortened cell lifetimes. Due to the high stability of the LTO and the capacitive oversizing of the NMC, no strong influence on aging is to be expected from the shift of the used potential ranges. This is consistent with the available measurement data.

Regarding the internal resistance the PEE has no quantifiable influence. On the one hand, at high temperatures prevailing in the test, the equalization process is largely completed by the second check-up. On the other hand, the internal resistance of the tested LTO/NMC cell is nearly SOC independent in the SOC range between 5 % and 95 % at 25 °C.

For a systematically analysis of cell aging, the PEE must be considered and quantified in the test design. At best, the cells have to be long-time stored at a defined storage SOC prior to test start, if no information on the history of the cells is available. If a determination of the geometric arrangement within the cell is impossible, methodologies as described by Lewerenz et al. [32] and Warnecke et al. [33] enable a rough quantification of the share of passive area. In the application context, the resulting inac-

curacies can cause significant misjudgments regarding the remaining capacity. However, it should be mentioned at this point that the standard transport of lithium-ion batteries is carried out at SOCs between 30% and 50% and that the average SOC in application operation is often in the medium SOC range. This leads to lower deviations and calculation errors. To reduce the impact of the PEE, one goal of cell design should be to minimize the overhang.

3.1.2. Temperature dependence

The examined LTO/NMC cells show a clear temperature dependency only with regard to the increase in internal resistance. As shown in Figure 5a, the cells perform identically at 40 °C and 60 °C in terms of capacity retention. After more than 300 days of testing, approximately 100% of the initial capacity is still available. The capacity of the cell stored at 80 °C increases to about 105 % before the cell had to be removed from the test due to bursting of the pouch bag, caused by strong gassing behaviour. The PEE does not explain the sharp and continuous rise in capacity for two reasons. Firstly, all 3 cells had a similar initial state between 2.11 to 2.124 V before the test started. Secondly, according to the theory of the PEE, the subsequent calendar aging phase at 55 %, which corresponds approximately to 2.2 V, should lead to a slight decrease in available capacity. In the examined cell, the LTO material determines the cell capacity due to the cell balancing. Perhaps the gassing behavior causes increased pressure within the LTO active material and in consequence cracking, which leads to an increase of the active surface area ('electrochemical milling') [34, 35, 36]. A permanent structural change of the LTO material due to the high ambient temperature may also be conceivable. Further investigations will try to substantiate the observed behaviour.

Regarding the internal resistance increase, presented in Figure 5b, the 3 tested cells indicate significant differences depending on the storage temperature. The inter-

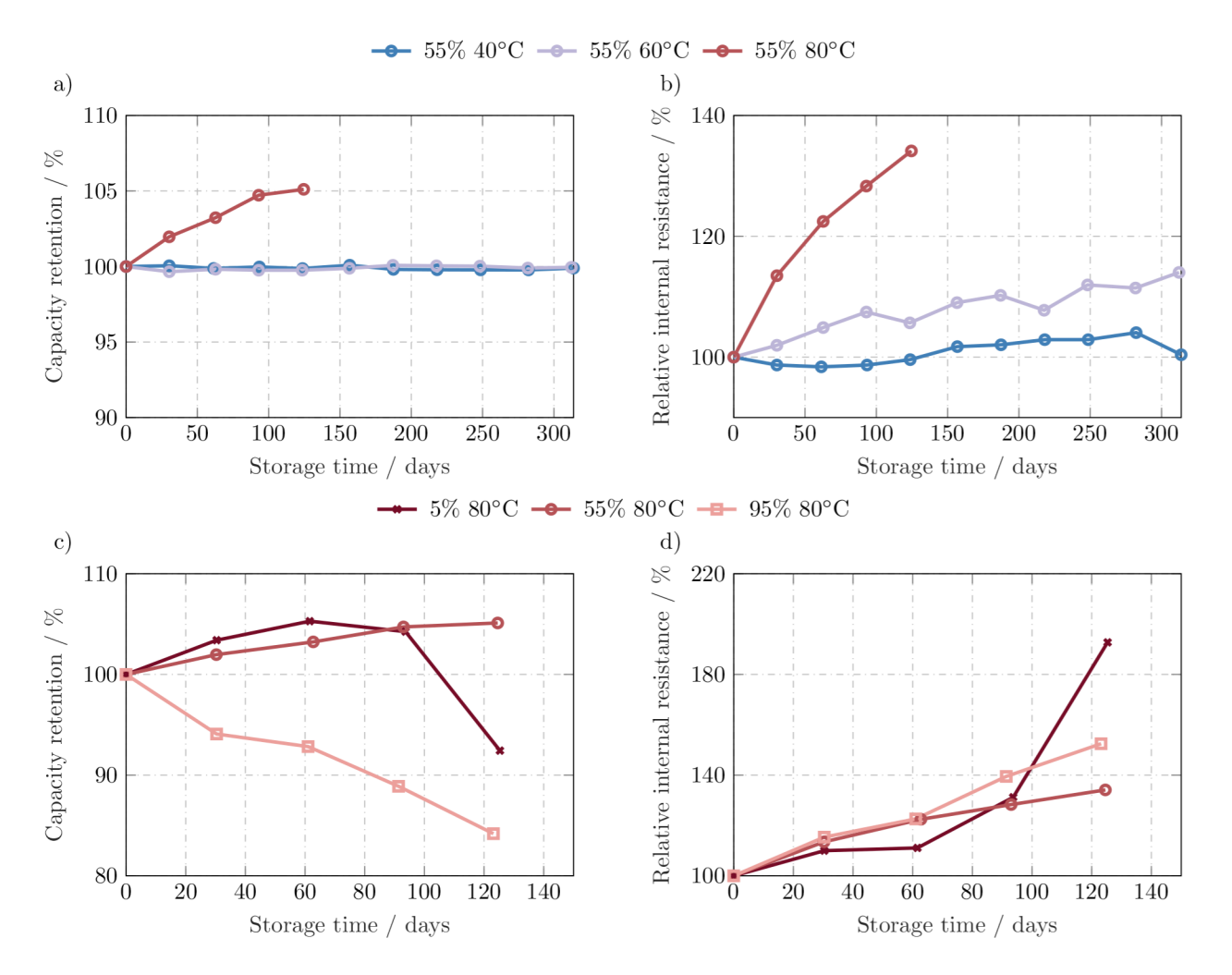


Figure 5: a) Normalized capacity over time and b) normalized resistance over time for calendar aging tests at 55 % SOC and different temperatures. Only the cell at 80 °C shows a change in capacity. The resulting internal resistances suggest a temperature dependency. c) Normalized capacity over time and d) normalized resistance over time for calendar aging tests at 80 °C and different SOC. Due to strong gassing behavior, all three cells show a large increase in internal resistance. The cells were removed from the test after the pouch bag film had burst.

nal resistance of the cell at 40 °C increases by 5% in the observation period of 240 days, at 60 °C by 14% and at 80 °C after 120 days even by 35%. Considering the strong gassing behaviour of the cell at 80 °C up to venting, the internal resistance increase is low and a good cell performance is still given. The continuous compression of the cells allows a large part of the gases produced to be displaced into the peripheral areas where the gas reservoirs are located. Assuming an Arrhenius dependency, the relationship between temperature and internal resistance rise

is usable for aging simulations and lifetime predictions.

${\it 3.1.3. Cell performance under severely high temperatures}$

At very high temperatures the LTO/NMC cells SOC independently show a strong gassing behaviour, with both the upper and lower SOC range being particularly critical. Figure 5c and d show the capacity and internal resistance curves of the cells stored at 80 °C. As 80 °C corresponds to the highest storage temperature approved by the cell manufacturer, it is not to be described as an abuse scenario. In the first 60 days, both the PEE and the previously de-

scribed abnormal behaviour at 55 % SOC predominate in relation to the residual capacity. At this point, the capacities of the cells stored at 5 % SOC and 95 % SOC decrease significantly. A possible reason for this could be a loss of contact within the cell caused by gassing [24]. This loss of contact could be caused by electrolyte displacement on the one hand and by cracking of the active material on the other hand. This theory coincides with the significant increase in internal resistance from 60 days test duration for cells with 5 % SOC and 95 % SOC. For these two cells a direct correlation between residual capacity and internal resistance increase exists. With respect to the internal resistance, the cell stored at 55 % SOC appears to be the least noticeable.

As already postulated in [8, 37], the results suggest that different gassing reactions take place within the cell depending on the state of charge. However, such a strong gassing in low SOC areas has not been observed so far. It remains to be investigated which electrochemical reaction at which of the two active materials is mainly responsible for the detected gassing behaviour. Generally, when using the cells in an application, temperatures beyond 70 °C should be avoided for safety reasons in order to prevent the cells from swelling or, in extreme cases, venting. In addition to high states of charge, which are often described as critical to the battery life time, the focus should also be on low states of charge in combination with high temperatures and taken into account in the operating strategy.

3.2. Cyclic aging

In the following observations, mostly results of the change in residual capacities are shown. This is due to the fact that the measured internal resistances often do not show a clear aging trend. Especially the cyclic aging tests at 40 °C do not lead to a significant increase of the internal resistance. In addition, despite the 4-pole measuring principle, measuring inaccuracies are still present due to the extremely low internal resistances of the LTO/NMC cells.

The number of equivalent full cycles is calculated on the basis of the available capacity in the first check-up before test start. All cycle tests, including the SOC setting at test start and at SOC reset, were Ah-based. The initial loss of capacity observed in all tests from Table 4 is, to our knowledge, attributable to the PEE. The cells in these cyclic aging tests had a state of charge between 2.111 to $2.124\,\mathrm{V}$ prior to test start, so that at an average SOC of $50\,\%$ or $55\,\%$ an initial drop in usable capacity is expected. For this reason, the phenomenon is not addressed in every illustration.

3.2.1. Influence of cycle depth on cell aging

Despite the "zero-strain" property of LTO, the aging behavior of the examined cells reveals a clear dependence on the cycle depth. For 40 °C and 60 °C the residual capacity curves for different cycle depths are shown in Figure 6a and b. For the 40 °C tests (see Figure 6a), significant differences between the cycle depths 100%, 70% and the rest are apparent. Small cycle depths $(\Delta \text{DOD} \leq 20\%)$ only lead to a slight loss of capacity, whereas full cycles accelerate the aging process by a large factor. Taking into account an end-of-life criterion for the remaining capacity of 80%, the cell with 100% ΔDOD has an estimated cycle life of approximately 20,000 equivalent full cycles. This number is considerable under the present boundary conditions $(40\,^{\circ}\text{C}, 5\text{C}/5\text{C}, 100\% \Delta \text{DOD})$.

At 60 °C, see Figure 6b, the cell at 70 % ages in a comparable order of magnitude. Interestingly, the cell with a cycle depth of 70 % and an overlaid sawtooth profile of 2 % Δ DOD shows a significantly lower aging rate. Nevertheless, this rate is stronger than that of the cell cycled at 5 % DOD. On the one hand, this demonstrates that lower cycle depths generally lead to lower stress for the examined cell. On the other hand, it allows the assumption that the cell exhibits an SOC dependent aging behavior at least in the range between 20 % and 90 %. A more detailed consideration of this will be presented in the further course of

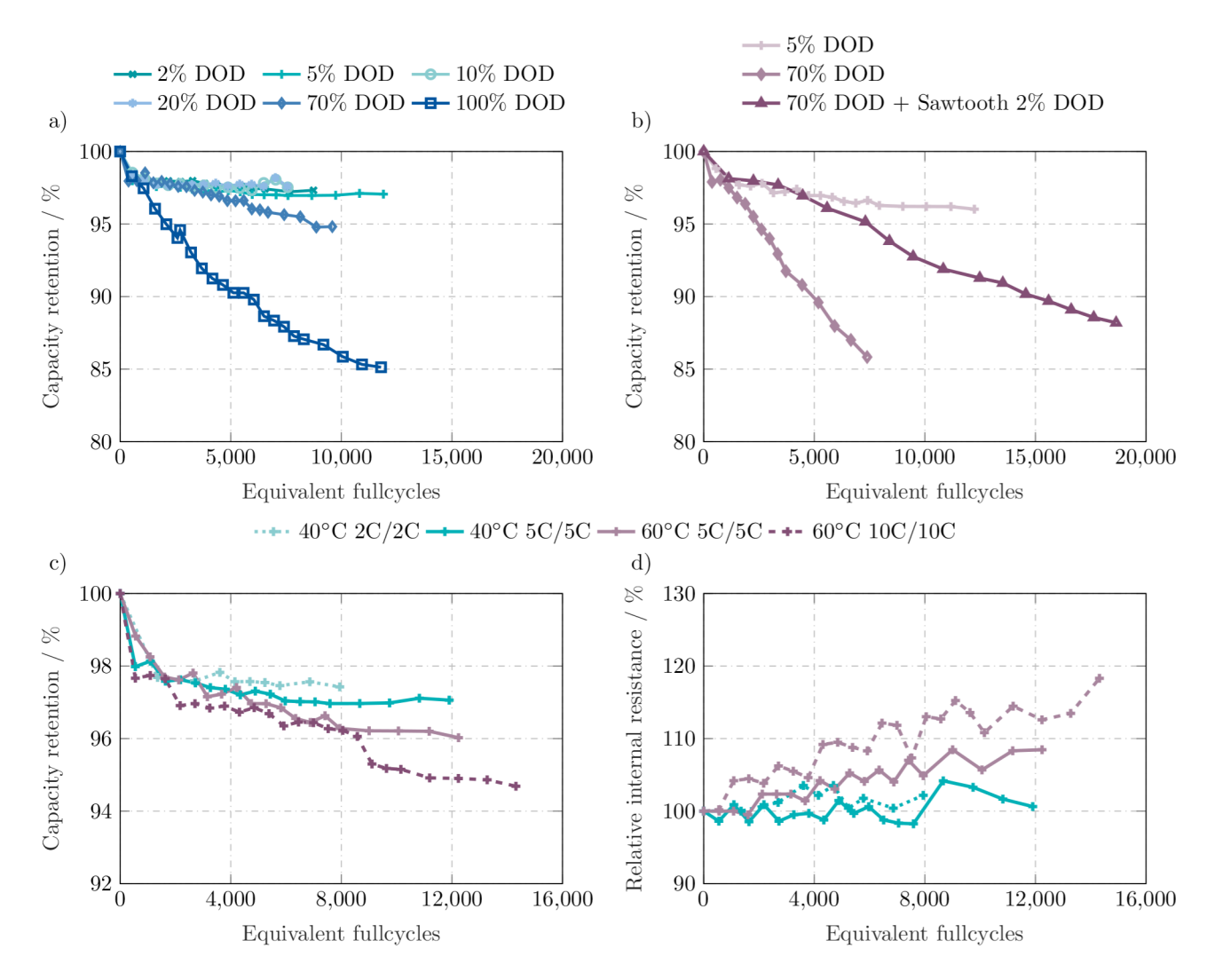


Figure 6: Normalized capacity over time for calendar aging tests with different cycle depths at a) 40 °C and b) 60 °C. With increasing cycle depths the impact on the aging behavior in terms of capacity degradation rises. c) Normalized capacity and d) normalized resistance over equivalent full cycles cyclic aging tests at 40 °C and 60 °C with three different current rates and 5 % Δ DOD. An influence of the current rate as well as the temperature on the aging behaviour is noticeable. The self-heating of the cells is very low due to low internal resistances and good heat dissipation via the pressure plates.

this work. The LTO/NMC cell offers an excellent life time when cycled in medium SOC ranges (SOC_{mean}). However, the results illustrate the difficulties associated with aging tests of LTO-based cells. Despite an operating point just below the maximum allowed temperature limit (70 °C at cyclization), high current testing is necessary to allow a test period of a few months to a few years. This leads to high costs for test bench occupation and also requires parallelisation of test equipment, depending on the cell size.

3.2.2. Influence of current rate on cell aging

Based on the existing results, the stress factor current cannot be clearly classified as life time shortening. In Figure 6c the remaining capacity of two cells is shown, which were loaded with two C-rates each and two different test temperatures at 5% ΔDOD . The capacity loss after the first capacity drop caused by the PEE can be described as approximately linear for all cells. After 12,000 equivalent full cycles, the 10C/10C current load causes approx-

imately 20% more capacity loss than the 5C/5C cycles, however, this corresponds only to 1% capacity difference. The different self-heating of the cells at the various current rates must be taken into account. These were 0 to 2°C at 2C/2C, 2 to 4°C at 5C/5C and 4 to 6°C at 10C/10C. As shown in Figure 5a, this difference should not have a significant effect on the capacitive cell aging.

Regarding the internal resistance, see Figure 6d, the findings are similar. The increase in internal resistance does not exceed the calendar aging effect shown in Figure 5b over the period under consideration. Nevertheless, the 10C/10C seem to lead to a stronger increase compared to the 5C/5C at 60 °C. It is possible that cyclization could lead to greater current dependence at greater cycle depths, since the probability of concentration gradients in the active material increases. Nevertheless, the results are highly interesting in the application context and demonstrate the suitability of the investigated LTO/NMC cells for dynamic high-performance applications. Furthermore, the superior resistance to high current rates allows for accelerated aging tests in terms of overall energy throughput.

3.2.3. Influence of voltage level on cell aging

Low voltage ranges cause severe aging of the examined cells and should be considered at least as critical as high voltage ranges. As can be seen in Figure 7, the cells in the lower voltage range (2.0 to 2.4 V) show the strongest aging trend. As with calendar aging at low SOCs, the reason for this behavior is not clear. In the literature, accelerated ageing is often associated with high states of charge at cell level. This is reported for both lithiated LTO and delithiated NMC. Both states possess an increased reactivity and thus accelerate possible side reactions [8, 38]. However, first results of cell openings show significant cover layers on both electrodes even at low SOCs and elevated temperatures. Further investigations will try to characterize the SEI respectively electrolyte decomposition products and thus to find the cause of the accelerated aging behavior.

The PEE is clearly evident in the results presented. All cells in this test were stored at about 5 % SOC before test start. The differences of the cells cycled between 2.0 and 2.4 V in the first 500 cycles are due to an unintentional full charge phase of 2.5 and 4 days respectively prior to test start. This emphasizes the importance of the consideration of the cell history. Otherwise, misjudgements of in this case almost 4 % capacity difference are possible after a few hundred cycles. Therefore, if the history of the cells is unclear and a PEE could potentially be present, the aging trend should always be taken into account, neglecting the initial drop.

The upper cut-off voltage seems to have little influence on the aging rate. From the 1000th equivalent full cycle on, the cells with an upper voltage limit of 2.5 or 2.65 V age almost identical. With regard to the change in internal resistance, no differentiation between the tested voltage ranges is possible, partially because of the high scattering.

3.2.4. Aging by drive cycle

Aging with real drive cycles illustrates the positive effect of small cycle depths on the remaining cell capacity. As shown in Figure 8a, the three tested cells exhibit a similar capacity loss of less than 3% after almost 10,000 equivalent full cycles. On the one hand, this temperature-independence of the capacitive aging behavior corresponds to the results in Figure 5a. On the other hand, the aging impact of high pulse currents in connection with low cycle depths is small for the investigated LTO/NMC cells. Thus, achieving the application-relevant lifetime requirement of more than 27,000 equivalent full cycles, see [3], is not critical. The PEE described above is minor, since the cells were cycled on average in the middle SOC range and were previously stored at approximately 30% SOC.

The increase of the internal resistance is temperaturedependent and life-time-critical and should therefore be a prioritized criterion in battery development. All three cells experience a rise in internal resistance with increas-

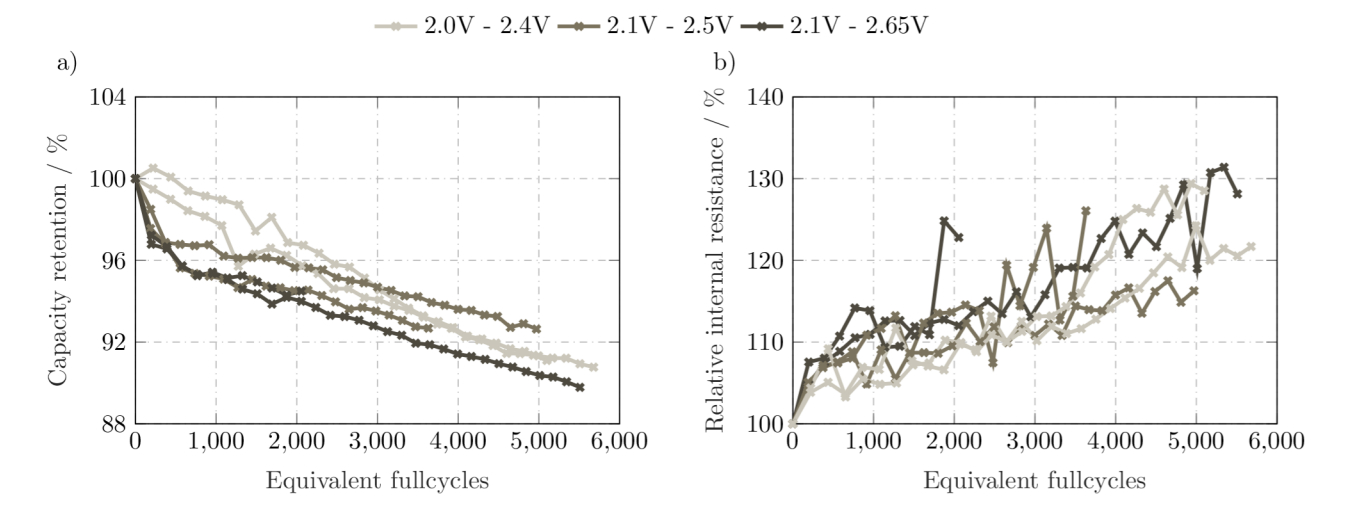
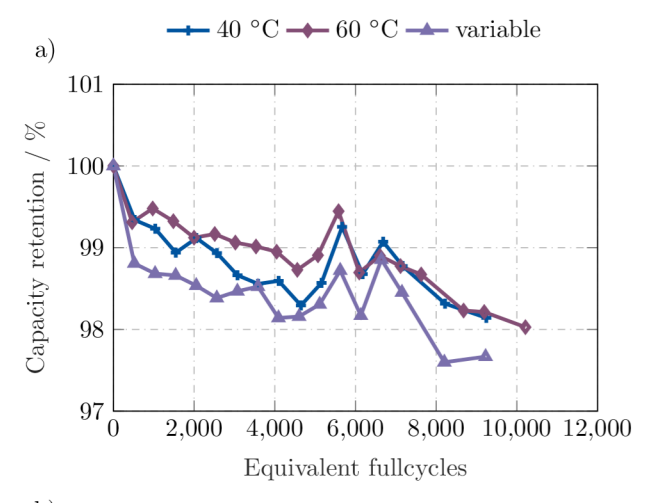


Figure 7: a) Normalized capacity over time and b) normalized resistance over time for cyclic aging tests at 60 °C, 5C/5C and different voltage ranges. The impact of the cut-off voltage is low. However, the rapidity of the capacity loss of cells cycled in lower voltage ranges is most critical. No distinct statement can be made regarding the increase in internal resistance.

ing number of equivalent full cycles shown in Figure 8b. The internal resistance of the cell at 60 °C increases about 3 times as much as the internal resistance of the cell at 40 °C. The reason for this may be accelerated and additional side reactions, which can lead, for example, to the formation of a covering layer on the electrodes or gassing. Since the results of the calendar aging tests, see Figure 5b, were quite similar, the cyclic stress seems to have only a negligible effect on the internal resistance. Interestingly, the cell with the variable temperature profile shows the largest increase, although the average temperature in this profile is below 40 °C. No explanation for this could be found so far. Perhaps the temperature changes have a negative effect on degradation. To exclude the risk of the cell being an outlier, additional measurements need to be carried out. Under the condition of a maximum increase of 50% over the battery life and the assumption of a linear progression, 27,000 equivalent full cycles are realistic. Depending on the ambient temperature within the application, special attention must therefore be paid to the internal resistance in the development process.

3.3. Resulting implications for 48 V applications

For the application-based context, the results of the aging tests have several, mostly positive, implications. On the one hand, it could be shown that small cycle depths, as they occur predominantly in 48 V applications, have a negligible impact on cell aging. No explicit deterioration in cell performance can be detected after deduction of calendar aging. In addition, other stress factors such as high current rates and high energy throughputs have a low influence on aging. It must be ensured that low and high states of charge are avoided, as these accelerate the aging process and, depending on the ambient temperature, gassing reactions. In spite of the high temperature stability of the tested cells, the ambient temperature in the application is decisive with regard to the increase in internal resistance. For this reason, special attention must be paid to the expected battery temperature in the development process. The high capacitive stability of the LTO/NMC cells can be used to minimize capacitive reserves, which serve to achieve the defined end-of-life performance. For example, a 10% reduction of the nominal capacity could be considered while simultaneously increasing the frequently used 80% end-of-life requirement. The opposite applies to the



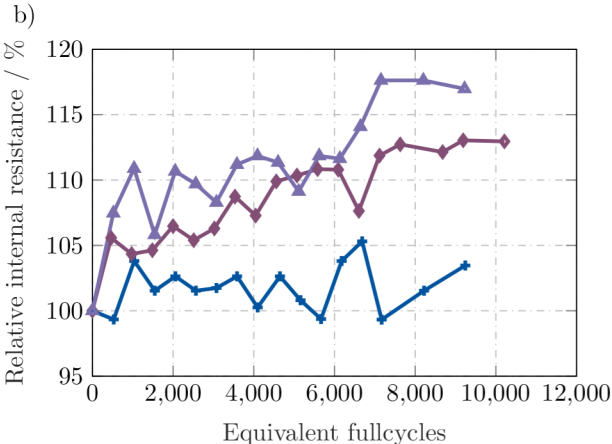


Figure 8: a) Normalized capacity over time and b) normalized resistance over time for drive cyclic aging tests at different ambient temperatures. The capacity retention is almost temperature independent. In contrast, the results for the internal resistances for the cells at 40 °C and 60 °C show a clear influence of temperature. The increased aging behaviour of the cell with variable temperature profile is surprising and cannot be explained so far.

internal resistance according to the illustrated cycle life results. When designing the cell it is essential to ensure that the end-of-life performance defined for the application is guaranteed. Since the calendar aging represents the more severe challenge for the examined cell in the application-related operation, relevant stress factors have to be minimized or greater reserves have to be ensured. It may be necessary to improve the battery cooling or to make cell-specific changes. The latter can be achieved by reducing the layer thickness of the electrodes or the thickness of the

separator.

4. Summary and Outlook

Quantifying the influential parameters relevant for battery aging in an 48 V system is necessary for a large-scale and error-free application in the vehicle. In this work, 33 state-of-the-art LTO/NMC cells were exposed to cyclic, calendar and drive cyclic aging regimes. The chosen load scenarios were derived previously from real vehicle data and therefore cover the application-relevant operating conditions of the cells in the vehicle.

The calendar aging tests indicated little to no loss of capacity at temperatures of less than or equal to 60 °C independent of the SOC. If a change in capacity was observed in the first weeks of the test, this was predominantly caused by the PEE. Importantly, the PEE is for the first time reported in a cell with geometrically oversized cathodes. A theoretical and descriptive explanatory model is presented, which highlights the unavoidable relocation of lithium-ions into and out of passive electrode areas. This relocation alters the initial cell balancing and thus explains the reversible loss or increase of capacity. The presented argumentation is transferable to graphite-based cells and shows, for example, the increased risk for lithium plating due to CV phases during cyclization.

Storage of cells at extremely high temperatures (80 °C) led to a strong gassing behavior, which occurred both at high and low states of charge. The latter has not been reported in the literature previously. In addition, under systematic cycling at lower voltage ranges a greater loss of capacity was observed. This confirmed the assumption that operation at lower voltage ranges triggers special aging processes.

Exposure to real drive cycles demonstrated the capacitive stability of the LTO/NMC cells. An increase in internal resistance, which was mainly influenced by calendar aging at high temperatures, was the lifetime-determining factor. Thus, with respect to cell development for a $48\,\mathrm{V}$

system, special attention must be paid to performance fulfillment at end-of-life.

In a next step, the aging results from this publication will serve as a data base for a parameterization of a semiempirical aging model. This will cover an open niche in the field of aging models for high power cells and in particular LTO/NMC based cells. Especially with regard to the PEE, a concrete breakdown of the impacts of cathode and anode is needed. In addition, it remains to be investigated how rapidly the concentration gradient between the active and passive area equalizes and how the effect can be adequately integrated into an aging model. Additional investigations will attempt to determine the cause of gassing within low states of charge. For this purpose, in-situ as well as exsitu methods on the half-cell level could be applied, which would allow for an identification of relevant side reactions.

5. Acknowledgment

We thank Dr. Nicholas Löffler, Nataliia Moskvina and Dr. Claudia Bank for fruitful discussions. This work was financially and technically supported by BMW AG. We would also like to thank BatterieIngenieure GmbH, who was responsible for the commissioning and test execution and who was always on hand to provide assistance.

References

- B. Mahr, 48 volt technology more than a mild hybrid,
 in: M. Bargende, H.-C. Reuss, J. Wiedemann (Eds.), 16. Internationales Stuttgarter Symposium, Proceedings, Springer Fachmedien Wiesbaden, Wiesbaden, 2016, pp. 1091–1100. doi: 10.1007/978-3-658-13255-2{\textunderscore}81.
- [2] A. Abdellahi, S. Khaleghi Rahimian, B. Blizanac, B. Sisk, Exploring the opportunity space for high-power li-ion batteries in next-generation 48v mild hybrid electric vehicles, in: SAE Technical Paper Series, SAE Technical Paper Series, SAE International 400 Commonwealth Drive, Warrendale, PA, United States, 2017. doi:10.4271/2017-01-1197.
- [3] T. Bank, S. Klamor, D. U. Sauer, Lithium-ion cell requirements in a real-world 48 v system and implications for an extensive aging analysis, Journal of Energy Storage 30 (2020) 101465. doi:10.1016/j.est.2020.101465.
 - URL http://www.sciencedirect.com/science/article/pii/ S2352152X20303303
- [4] B. Zhao, R. Ran, M. Liu, Z. Shao, A comprehensive review of li 4 ti 5 o 12 -based electrodes for lithium-ion batteries: The latest advancements and future perspectives, Materials Science and Engineering: R: Reports 98 (2015) 1-71. doi:10.1016/j. mser.2015.10.001.
- [5] X. Sun, P. V. Radovanovic, B. Cui, Advances in spinel li 4 ti 5 o 12 anode materials for lithium-ion batteries, New Journal of Chemistry 39 (1) (2015) 38–63. doi:10.1039/C4NJ01390E.
- [6] Z. Chen, I. Belharouak, Y.-K. Sun, K. Amine, Titanium-based anode materials for safe lithium-ion batteries, Advanced Functional Materials 23 (2013). doi:10.1002/adfm.201200698.
- [7] S. S. Zhang, A review on electrolyte additives for lithium-ion batteries, Journal of Power Sources 162 (2) (2006) 1379–1394. doi:10.1016/j.jpowsour.2006.07.074.
- [8] W. Lv, J. Gu, Y. Niu, K. Wen, W. He, Review-gassing mechanism and suppressing solutions in li4ti5o12-based lithium-ion batteries, Journal of The Electrochemical Society 164 (9) (2017) A2213-A2224. doi:10.1149/2.0031712jes.
 - URL https://doi.org/10.1149%2F2.0031712jes
- [9] Y.-L. Ding, Z. Cano, A. Yu, J. Lu, Z. Chen, Automotive li-ion batteries: Current status and future perspectives, Electrochemical Energy Reviews (2019) 1–28doi:10.1007/s41918-018-0022-z.
- [10] N. Takami, H. Inagaki, Y. Tatebayashi, H. Saruwatari, K. Honda, S. Egusa, High-power and long-life lithium-ion batteries using lithium titanium oxide anode for automotive and stationary power applications, Journal of Power Sources 244 (2013) 469–475. doi:10.1016/j.jpowsour.2012.11.055.
- [11] J. K. Yoon, S. Nam, H. C. Shim, K. Park, T. Yoon, H. S. Park,

- S. Hyun, Highly-stable li_4ti_5o12 anodes obtained by atomic-layer-deposited al_2o_3 , Materials (Basel, Switzerland) 11 (5) (2018). doi:10.3390/ma11050803.
- [12] N. Nitta, F. Wu, J. T. Lee, G. Yushin, Li-ion battery materials: present and future, Materials Today 18 (5) (2015) 252–264. doi: 10.1016/j.mattod.2014.10.040.
- [13] F. Hall, J. Touzri, S. Wußler, H. Buqa, W. G. Bessler, Experimental investigation of the thermal and cycling behavior of a lithium titanate-based lithium-ion pouch cell, Journal of Energy Storage 17 (2018) 109-117. doi:10.1016/j.est.2018.02.012.
- [14] X. Han, M. Ouyang, L. Lu, J. Li, Cycle life of commercial lithium-ion batteries with lithium titanium oxide anodes in electric vehicles, Energies 7 (8) (2014) 4895–4909. doi: 10.3390/en7084895.
- [15] A.-I. Stroe, D.-I. Stroe, V. Knap, M. Swierczynski, R. Teodorescu, D.-L. Stroe, Accelerated lifetime testing of high power lithium titanate oxide batteries, in: 2018 IEEE Energy Conversion Congress and Exposition (ECCE), 2018, pp. 3857–3863. doi:10.1109/ECCE.2018.8557416.
- [16] P. Svens, R. Eriksson, J. Hansson, M. Behm, T. Gustafsson, G. Lindbergh, Analysis of aging of commercial composite metal oxide – li 4 ti 5 o 12 battery cells, Journal of Power Sources 270 (2014) 131–141. doi:10.1016/j.jpowsour.2014.07.050.
- [17] M. Dubarry, N. Qin, P. Brooker, Calendar aging of commercial li-ion cells of different chemistries – a review, Current Opinion in Electrochemistry 9 (2018) 106–113. doi:10.1016/j.coelec. 2018.05.023.
- [18] C. R. Fell, L. Sun, P. B. Hallac, B. Metz, B. Sisk, Investigation of the gas generation in lithium titanate anode based lithium ion batteries, Journal of The Electrochemical Society 162 (9) (2015) A1916-A1920. doi:10.1149/2.1091509jes.
- [19] M. Winter, J. Besenhard, M. Spahr, P. Novak, Insertion electrode materials for rechargeable lithium batteries, Advanced Materials 10 (1998) 725.
- [20] J. Schmalstieg, S. Käbitz, M. Ecker, D. U. Sauer, A holistic aging model for li(nimnco)o2 based 18650 lithium-ion batteries, Journal of Power Sources 257 (2014) 325-334. doi:10.1016/j. jpowsour.2014.02.012.
- [21] M. Lewerenz, S. Käbitz, M. Knips, J. Münnix, J. Schmalstieg, A. Warnecke, D. U. Sauer, New method evaluating currents keeping the voltage constant for fast and highly resolved measurement of arrhenius relation and capacity fade, Journal of Power Sources 353 (2017) 144–151. doi:10.1016/j.jpowsour. 2017.03.136.
- [22] A. Marongiu, F. Nußbaum, W. Waag, M. Garmendia, D. Sauer, Comprehensive study of the influence of aging on the hysteresis behavior of a lithium iron phosphate cathode-based lithium ion battery – an experimental investigation of the hysteresis, Ap-

- plied Energy 171 (2016) 629-645. doi:10.1016/j.apenergy. 2016.02.086.
- [23] A. Barai, W. D. Widanage, J. Marco, A. McGordon, P. Jennings, A study of the open circuit voltage characterization technique and hysteresis assessment of lithium-ion cells, Journal of Power Sources 295 (2015) 99–107. doi:10.1016/j.jpowsour. 2015.06.140
- [24] J. Vetter, P. Novák, M. R. Wagner, C. Veit, K.-C. Möller, J. O. Besenhard, M. Winter, M. Wohlfahrt-Mehrens, C. Vogler, A. Hammouche, Ageing mechanisms in lithium-ion batteries, Journal of Power Sources 147 (1-2) (2005) 269–281. doi: 10.1016/j.jpowsour.2005.01.006.
- [25] M. Broussely, P. Biensan, F. Bonhomme, P. Blanchard, S. Herreyre, K. Nechev, R. J. Staniewicz, Main aging mechanisms in li ion batteries, Journal of Power Sources 146 (1-2) (2005) 90-96. doi:10.1016/j.jpowsour.2005.03.172.
- [26] X. Han, L. Lu, Y. Zheng, X. Feng, Z. Li, J. Li, M. Ouyang, A review on the key issues of the lithium ion battery degradation among the whole life cycle, eTransportation 1 (2019) 100005. doi:10.1016/j.etran.2019.100005.
- [27] B. Gyenes, D. A. Stevens, V. L. Chevrier, J. R. Dahn, Understanding anomalous behavior in coulombic efficiency measurements on li-ion batteries, Journal of The Electrochemical Society 162 (3) (2015) A278-A283. doi:10.1149/2.0191503jes.
- [28] M. Lewerenz, J. Münnix, J. Schmalstieg, S. Käbitz, M. Knips, D. U. Sauer, Systematic aging of commercial lifepo 4 —graphite cylindrical cells including a theory explaining rise of capacity during aging, Journal of Power Sources 345 (2017) 254–263. doi:10.1016/j.jpowsour.2017.01.133.
- [29] T. Hüfner, M. Oldenburger, B. Bedürftig, A. Gruhle, Lithium flow between active area and overhang of graphite anodes as a function of temperature and overhang geometry, Journal of Energy Storage 24 (2019) 100790. doi:10.1016/j.est.2019. 100790.
- [30] X. Wu, K. Song, X. Zhang, N. Hu, L. Li, W. Li, L. Zhang, H. Zhang, Safety issues in lithium ion batteries: Materials and cell design, Frontiers in Energy Research 7 (2019) 65. doi: 10.3389/fenrg.2019.00065.
 - URL https://www.frontiersin.org/article/10.3389/fenrg.
- [31] F. Grimsmann, T. Gerbert, F. Brauchle, A. Gruhle, J. Parisi, M. Knipper, Hysteresis and current dependence of the graphite anode color in a lithium-ion cell and analysis of lithium plating at the cell edge, Journal of Energy Storage 15 (2018) 17–22. doi:10.1016/j.est.2017.10.015.
- [32] M. Lewerenz, G. Fuchs, L. Becker, D. U. Sauer, Irreversible calendar aging and quantification of the reversible capacity loss caused by anode overhang, Journal of Energy Storage 18 (2018)

- 149-159. doi:10.1016/j.est.2018.04.029.
- [33] A. J. Warnecke, Degradation mechanisms in nmc-based lithium-ion batteries, Dissertation, RWTH Aachen University, Aachen (2017). doi:10.18154/RWTH-2017-09646. URL https://publications.rwth-aachen.de/record/ 708098RWTH
- [34] M. Dubarry, C. Truchot, B. Y. Liaw, Cell degradation in commercial lifepo4 cells with high-power and high-energy designs, Journal of Power Sources 258 (2014) 408-419. doi:10.1016/j.jpowsour.2014.02.052.
- [35] S. Chauque, F. Oliva, A. Visintin, D. Barraco Diaz, E. Leiva, O. R. Cámara, Lithium titanate as anode material for lithium ion batteries: Synthesis, post-treatment and its electrochemical response, Journal of Electroanalytical Chemistry 799 (2017). doi:10.1016/j.jelechem.2017.05.052.
- [36] J. Christensen, Modeling diffusion-induced stress in li-ion cells with porous electrodes, Journal of The Electrochemical Society 157 (3) (2010) A366. doi:10.1149/1.3269995.
 URL https://doi.org/10.1149%2F1.3269995
- [37] M. He, E. Castel, A. Laumann, G. Nuspl, P. Novák, E. J. Berg, In situ gas analysis of li 4 ti 5 o 12 based electrodes at elevated temperatures, Journal of The Electrochemical Society 162 (6) (2015) A870–A876. doi:10.1149/2.0311506jes.
- [38] F. Schipper, E. M. Erickson, C. Erk, J.-Y. Shin, F. F. Chesneau, D. Aurbach, Review\textemdashrecent advances and remaining challenges for lithium ion battery cathodes, Journal of The Electrochemical Society 164 (1) (2016) A6220-A6228. doi:10.1149/2.0351701jes.
 - URL https://doi.org/10.1149%2F2.0351701jes